SCIENCE CHINA
Technological Sciences

July 2010 Vol.53 No.7: 1904–1912
doi: 10.1007/s11431-010-3185-3

Third-order point contact approach for five-axis sculptured surface machining using non-ball-end tools (I): Third-order approximation of tool envelope surface

ZHU LiMin[1*], DING Han[2] & XIONG YouLun[2]

[1] *State Key Laboratory of Mechanical System and Vibration, Shanghai Jiao Tong University, Shanghai 200240, China;*
[2] *State Key Laboratory of Digital Manufacturing Equipment and Technology, Huazhong University of Science and Technology, Wuhan 430074, China*

Received September 3, 2009; accepted December 24, 2009

In this paper, the geometric properties of a pair of line contact surfaces are investigated. Then, based on the observation that the cutter envelope surface contacts with the cutter surface and design surface along the characteristic curve and cutter contact (CC) path, respectively, a mathematical model describing the third-order approximation of the cutter envelope surface according to just one given cutter location (CL) is developed. It is shown that at the CC point both the normal curvature of the normal section of the cutter envelope surface and its derivative with respect to the arc length of the normal section can be determined by those of the cutter surface and design surface. This model characterizes the intrinsic relationship among the cutter surface, cutter envelope surface and design surface in the neighborhood of the CC point, and yields the mathematical foundation for optimally approximating the cutter envelope surface to the design surface by adjusting the cutter location.

five-axis NC machining, rotary cutter, cutter envelope surface, normal curvature, third-order point contact

Citation: Zhu L M, Ding H, Xiong Y L. Third-order point contact approach for five-axis sculptured surface machining using non-ball-end tools (I): Third-order approximation of tool envelope surface. Sci China Tech Sci, 2010, 53: 1904–1912, doi: 10.1007/s11431-010-3185-3

1 Introduction

Sculptured or free-form surfaces are widely used in manufacturing industries. Automation of the manufacturing process from the nominal part geometry on a CAD system to the final machined part offers the opportunity for huge gains in productivity and cost savings. By promoting CNC machine tools from three-axis to five-axis, a significant improvement in efficiency and accuracy has been achieved for free-form surface machining. However, it is more difficult to position the cutter due to the two additional degrees of freedom. Nowadays, ball-end cutters are widely employed for five-axis NC machining. The major advantages of ball-end milling are that it applies to almost any surface and it is relatively easy to generate the tool path. Form the manufacturer's point of view, however, the main disadvantage of ball-end milling is that it is very time consuming. It may require more finish passes and each pass removes only a small amount of material. Compared with ball-end cutter, non-ball-end cutter possesses more complex geometry, and exhibits different "effective cutting profiles" at different locations. Thus, it is possible to position the cutter so that its "effective cutting profile" well matches the design surface, which results in a great improvement of the machining strip width. Hence, increasing attention has been drawn onto the problem of tool path optimization for milling complex surfaces with non-ball-end cutters.

In five-axis machining, the machined surface is formed by the swept envelope of the cutter surface. The true ma-

*Corresponding author (email: zhulm@sjtu.edu.cn)

chining errors are the deviations between the design surface and cutter envelope surface. It is impossible to determine the complete shape of the cutter envelope surface unless all the cutter positions are given [1, 2]. Therefore, how to evaluate the deviations between the cutter envelope surface and design surface when given only one cutter position is of great importance for individual cutter location planning. It determines the geometric accuracy of the finally machined surface. Due to the difficulty and complexity in modeling locally the cutter envelope surface, most works adopted the approximate or simplified models, which formulate the problem of optimal cutter positioning as that of approximating the cutter surface to the design surface in the neighborhood of the designated CC point [3–10]. However, these optimization models do not characterize the real machining process. Also, they only apply to certain surfaces or cutters.

So far, only a few works have addressed the cutter positioning problem from the perspective of local approximation of cutter envelope surface to design surface. Wang et al. [11] presented a curvature catering method for machining sculptured surfaces using disc cutters with concave ends. The cutter is positioned so that its envelope surface and the design surface have the same derivatives up to third order along the direction orthogonal to the cutting direction. Rao et al. [12] derived the expression of the curvature of the envelope surface of a flat-end cutter for local gouging detection and cutter orientation optimization. In these two works, the third- and second- order approximate models of the cutter envelope surface were developed, respectively. However, for a flat-end or disc cutter, its envelope surface is swept by the tool nose, which is a circle, not a rotary surface. Therefore, the two methods can not be extended to other types of rotary cutters, such as fillet-end cutter, cylindrical cutter, conical cutter, etc. Yoon et al. [13] introduced the Dupin indicatrix to characterize the envelope surface of a fillet-end cutter around the CC point. They pointed out that the Dupin indicatrix of the cutter envelope surface was tangent to those of the design surface and cutter surface. However, they did not discuss how to calculate this Dupin indicatrix. Recently, Gong et al. [14] developed a mathematical model that describes the second-order approximation of the envelope surface of a general rotary cutter in the neighborhood of the CC point, and then proposed a cutter positioning strategy that makes the cutter envelope surface have a contact of second-order with the design surface at the CC point. However, theoretically speaking, third-order contact between the cutter envelope surface and design surface could be achieved by adjusting the cutter orientation. This means that cutter location planning based on the second-order model does not take full advantage of the efficiency and power that five-axis machining offers.

In this paper, based on the observation that the cutter envelope surface contacts with the cutter surface and design surface along the characteristic curve and CC path respectively, an approach for third-order reconstruction of the cutter envelope surface using the normal curvatures and geodesic torsions of the cutter and design surfaces at the CC point is proposed. The remainder of this paper is organized as follows. In Section 2, the geometric properties of a pair of line contact surfaces are explored. In Section 3, the mathematical model describing the third-order approximation of the cutter envelope surface according to just one given CL is developed. In Section 4, the special case that the cutter surface degenerates into a circle is discussed. Section 5 concludes the paper.

2 Geometric foundation

2.1 Surface curve

As shown in Figure 1, the cutter surface keeps single point contact with the design surface during five-axis machining. The cutter surface, cutter envelope surface and design surface share the common CC point with the same tangent plane. A local coordinate frame $\boldsymbol{O}$-xyz is set up at the current CC point $\boldsymbol{r}_0$. Its x- and y-axes lie on the common tangent plane, and its z-axis is along the common normal.

In the local coordinate frame, the cutter surface, cutter envelope surface and design surface can be described by height functions $z^{(i)}(x, y)$, i=0, 1, 2, respectively, or represented in the following parametric forms,

$$\boldsymbol{r}^{(i)}(x,y)=\begin{bmatrix} x \\ y \\ z^{(i)}(x,y) \end{bmatrix} \quad (i=0,\ 1,\ 2). \tag{1}$$

Since the z-axis of the frame coincides with the common surface normal, it is easily verified that

$$z_x^{(i)}(0,0)=z_y^{(i)}(0,0)=0 \quad (i=0,\ 1,\ 2). \tag{2}$$

Denote by $\boldsymbol{r}^{(i)}(s)$ the curve on surface $\boldsymbol{r}^{(i)}$ that passes through point $\boldsymbol{r}_0$, where parameter s stands for the arc length of the curve measured from point $\boldsymbol{r}_0$, then we have

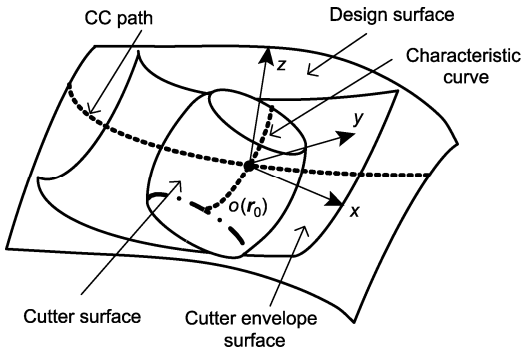

Figure 1 Point contact among the cutter surface, cutter envelope surface and design surface.

$$\frac{\mathrm{d}^2\boldsymbol{r}^{(i)}}{\mathrm{d}s^2}\cdot\boldsymbol{n}^{(i)}=\kappa_n^{(i)}=\frac{1}{\sqrt{1+(z_x^{(i)})^2+(z_y^{(i)})^2}}\times\left[z_{xx}^{(i)}(x_s)^2+2z_{xy}^{(i)}x_sy_s+z_{yy}^{(i)}(y_s)^2\right], \tag{3}$$

$$\frac{\mathrm{d}^3\boldsymbol{r}^{(i)}}{\mathrm{d}s^3}\cdot\boldsymbol{n}^{(i)}=\frac{1}{\sqrt{1+(z_x^{(i)})^2+(z_y^{(i)})^2}}\times\left[z_{xxx}^{(i)}(x_s)^3+3z_{xxy}^{(i)}(x_s)^2y_s+3z_{xyy}^{(i)}x_s(y_s)^2+z_{yyy}^{(i)}(y_s)^3+3z_{xx}^{(i)}x_sx_{ss}+3z_{xy}^{(i)}x_{ss}y_s+3z_{xy}^{(i)}x_sy_{ss}+3z_{yy}^{(i)}y_sy_{ss}\right], \tag{4}$$

where $\boldsymbol{n}^{(i)}$ denotes the unit normal vector of surface $\boldsymbol{r}^{(i)}$. If $\boldsymbol{r}^{(i)}(s)$ represents a normal section of surface $\boldsymbol{r}^{(i)}$ at point $\boldsymbol{r}_0$, we have

$$\frac{\mathrm{d}^2\boldsymbol{r}^{(i)}}{\mathrm{d}s^2}\cdot\frac{\mathrm{d}\boldsymbol{n}^{(i)}}{\mathrm{d}s}\Big|_{s=0}=0, \tag{5}$$

$$\dot{\kappa}_n^{(i)}\Big|_{s=0}=\frac{\mathrm{d}}{\mathrm{d}s}\left(\frac{\mathrm{d}^2\boldsymbol{r}^{(i)}}{\mathrm{d}s^2}\cdot\boldsymbol{n}^{(i)}\right)\Big|_{s=0}=\frac{\mathrm{d}^3\boldsymbol{r}^{(i)}}{\mathrm{d}s^3}\cdot\boldsymbol{n}^{(i)}\Big|_{s=0}, \tag{6}$$

$$\dot{\kappa}^{(i)}\Big|_{s=0}=\frac{\mathrm{d}}{\mathrm{d}s}\left(\frac{\mathrm{d}^2\boldsymbol{r}^{(i)}}{\mathrm{d}s^2}\cdot\frac{\mathrm{d}^2\boldsymbol{r}^{(i)}}{\mathrm{d}s^2}\right)^{\frac{1}{2}}\Big|_{s=0}=\frac{\mathrm{d}^3\boldsymbol{r}^{(i)}}{\mathrm{d}s^3}\cdot\boldsymbol{N}^{(i)}\Big|_{s=0}, \tag{7}$$

where $\boldsymbol{N}^{(i)}$ denotes the principal unit normal vector of the normal section $\boldsymbol{r}^{(i)}(s)$ at point $\boldsymbol{r}_0$. It is obvious that $\boldsymbol{n}^{(i)}=\pm\boldsymbol{N}^{(i)}$, which results in $\kappa_n^{(i)}\big|_{s=0}=\pm\kappa^{(i)}\big|_{s=0}$ and $\dot{\kappa}_n^{(i)}\big|_{s=0}=\pm\dot{\kappa}^{(i)}\big|_{s=0}$. The choice of plus or minus sign depends on the direction of $\boldsymbol{n}^{(i)}$, pointing to or away from the center of curvature of $\boldsymbol{r}^{(i)}(s)$. If $\kappa_n^{(i)}$ and $\dot{\kappa}_n^{(i)}$ are evaluated at point $\boldsymbol{r}_0$, after algebraic simplification we get

$$\kappa_n^{(i)}\big|_\alpha=z_{xx}^{(i)}\cos^2\alpha+2z_{xy}^{(i)}\cos\alpha\sin\alpha+z_{yy}^{(i)}\sin^2\alpha\big|_{x=0,y=0}, \tag{8}$$

$$\dot{\kappa}_n^{(i)}\big|_\alpha=z_{xxx}^{(i)}\cos^3\alpha+3z_{xxy}^{(i)}\cos^2\alpha\sin\alpha+3z_{xyy}^{(i)}\cos\alpha\sin^2\alpha+z_{yyy}^{(i)}\sin^3\alpha\big|_{x=0,y=0}, \tag{9}$$

where α is the angle between the tangent of $\boldsymbol{r}^{(i)}(s)$ at $\boldsymbol{r}_0$ and the x-axis of the local frame, $\kappa_n^{(i)}\big|_\alpha$ is the normal curvature of the normal section determined by angel α at point $\boldsymbol{r}_0$, and $\dot{\kappa}_n^{(i)}\big|_\alpha$ is its derivative with respect to the arc length of the normal section. Easily, we find that $z_{xxx}^{(i)}\big|_{x=0,y=0}$ and $z_{yyy}^{(i)}\big|_{x=0,y=0}$ are the derivatives of the normal curvatures of the two normal sections determined by x-z and y-z planes, respectively.

2.2 Contact order between two surfaces

In differential geometry, contact order is introduced to evaluate the approximation of two point contact surfaces around the contact point. Two curves $\boldsymbol{r}^{(i)}(s)$ and $\boldsymbol{r}^{(j)}(s)$ possess contact of order k at a common point $\boldsymbol{r}_0=\boldsymbol{r}^{(i)}(s_0)=\boldsymbol{r}^{(j)}(s_0)$ if they are regular at $\boldsymbol{r}_0$ and agree there in all derivatives up to the kth order. Accordingly, if two surfaces $\boldsymbol{r}^{(i)}$ and $\boldsymbol{r}^{(j)}$ share a common point $\boldsymbol{r}_0$ with the same tangent plane, a contact order can be calculated for each pair of normal sections obtained by intersecting the two surfaces with a plane containing the common surface normal at $\boldsymbol{r}_0$, as shown in Figure 2. The contact order between two surfaces is then defined as the minimal contact order between all pairs of normal sections.

According to the Taylor expansion of planar curves and the relationships that $\kappa_n^{(i)}=\pm\kappa^{(i)}$ and $\dot{\kappa}_n^{(i)}=\pm\dot{\kappa}^{(i)}$ at the point of interest, we get the following proposition.

Proposition 1. Assume that two surfaces $\boldsymbol{r}^{(i)}$ and $\boldsymbol{r}^{(j)}$ share a common point $\boldsymbol{r}_0$ with the same tangent plane. If $\kappa_n^{(i)}=\kappa_n^{(j)}$ holds along any tangent direction at point $\boldsymbol{r}_0$, then the two surfaces have at least the second-order contact. If $\kappa_n^{(i)}=\kappa_n^{(j)}$ and $\dot{\kappa}_n^{(i)}=\dot{\kappa}_n^{(j)}$ simultaneously hold along any tangent direction at point $\boldsymbol{r}_0$, then the two surfaces have at least the third-order contact.

2.3 Properties of a pair of line contact surfaces

Denote by $\boldsymbol{r}^{(1)}(s)=\boldsymbol{r}^{(i)}(s)$, i=0 or 2 the contact line between the cutter envelope surface and the cutter or design surface. The tangent vectors of the two surfaces at point $\boldsymbol{r}^{(1)}(s)=\boldsymbol{r}^{(i)}(s)$ have respectively the forms,

$$\mathrm{d}\boldsymbol{r}^{(1)}=\begin{bmatrix}1\\0\\z_x^{(1)}(s)\end{bmatrix}\mathrm{d}x+\begin{bmatrix}0\\1\\z_y^{(1)}(s)\end{bmatrix}\mathrm{d}y, \tag{10}$$

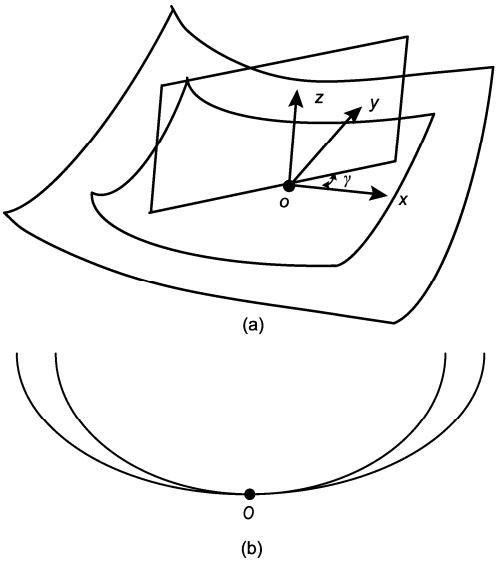

Figure 2 The pair of normal sections along the tangent direction determined by angel γ.

and

$$\mathrm{d}\boldsymbol{r}^{(i)} = \begin{bmatrix} 1 \\ 0 \\ z_x^{(i)}(s) \end{bmatrix} \mathrm{d}x + \begin{bmatrix} 0 \\ 1 \\ z_y^{(i)}(s) \end{bmatrix} \mathrm{d}y. \tag{11}$$

Since the two surfaces contact at point $\boldsymbol{r}^{(1)}(s)=\boldsymbol{r}^{(i)}(s)$, they share there the common tangent plane. As a result, we get

$$\begin{cases} z_x^{(1)}(s) = z_x^{(i)}(s), \\ z_y^{(1)}(s) = z_y^{(i)}(s). \end{cases} \tag{12}$$

Substituting eq. (12) into the identity $\dfrac{\mathrm{d}^2\boldsymbol{r}^{(1)}}{\mathrm{d}s^2}\cdot\boldsymbol{n}^{(1)} = \dfrac{\mathrm{d}^2\boldsymbol{r}^{(i)}}{\mathrm{d}s^2}\cdot\boldsymbol{n}^{(i)}$ results in

$$\begin{aligned} &z_{xx}^{(1)}(x_s)^2 + 2z_{xy}^{(1)}x_s y_s + z_{yy}^{(1)}(y_s)^2 \\ &\quad = z_{xx}^{(i)}(x_s)^2 + 2z_{xy}^{(i)}x_s y_s + z_{yy}^{(i)}(y_s)^2. \end{aligned} \tag{13}$$

Let s=0. It follows from eq. (8) that

$$\begin{aligned} \kappa_n^{(1)}\big|_\beta &= z_{xx}^{(1)}\cos^2\beta + 2z_{xy}^{(1)}\cos\beta\sin\beta + z_{yy}^{(1)}\sin^2\beta\big|_{x=0,y=0} \\ &= \kappa_n^{(i)}\big|_\beta = z_{xx}^{(i)}\cos^2\beta + 2z_{xy}^{(i)}\cos\beta\sin\beta + z_{yy}^{(i)}\sin^2\beta\big|_{x=0,y=0}, \end{aligned} \tag{14}$$

where β denotes the angle between the tangent of the contact line at $\boldsymbol{r}_0$ and the x-axis of the local frame.

Differentiating both sides of eq. (12) with respect to arc length s, we obtain

$$\begin{cases} z_{xx}^{(1)}x_s + z_{xy}^{(1)}y_s = z_{xx}^{(i)}x_s + z_{xy}^{(i)}y_s, \\ z_{yx}^{(1)}x_s + z_{yy}^{(1)}y_s = z_{yx}^{(i)}x_s + z_{yy}^{(i)}y_s. \end{cases} \tag{15}$$

Letting s=0, we have

$$\begin{cases} z_{xx}^{(1)}\cos\beta + z_{xy}^{(1)}\sin\beta\big|_{x=0,y=0} = z_{xx}^{(i)}\cos\beta + z_{xy}^{(i)}\sin\beta\big|_{x=0,y=0}, \\ z_{yx}^{(1)}\cos\beta + z_{yy}^{(1)}\sin\beta\big|_{x=0,y=0} = z_{yx}^{(i)}\cos\beta + z_{yy}^{(i)}\sin\beta\big|_{x=0,y=0}. \end{cases} \tag{16}$$

From eq. (15), we get

$$\begin{cases} z_{xx}^{(1)}x_s x_{ss} + z_{xy}^{(1)}y_s x_{ss} = z_{xx}^{(i)}x_s x_{ss} + z_{xy}^{(i)}y_s x_{ss}, \\ z_{yx}^{(1)}x_s y_{ss} + z_{yy}^{(1)}y_s y_{ss} = z_{yx}^{(i)}x_s y_{ss} + z_{yy}^{(i)}y_s y_{ss}. \end{cases} \tag{17}$$

Substituting eqs. (12) and (17) into the identity $\dfrac{\mathrm{d}^3\boldsymbol{r}^{(1)}}{\mathrm{d}s^3}\cdot\boldsymbol{n}^{(1)} = \dfrac{\mathrm{d}^3\boldsymbol{r}^{(i)}}{\mathrm{d}s^3}\cdot\boldsymbol{n}^{(i)}$ results in

$$\begin{aligned} &\left[z_{xxx}^{(1)}(x_s)^3 + 3z_{xxy}^{(1)}(x_s)^2 y_s + 3z_{xyy}^{(1)}x_s(y_s)^2 + z_{yyy}^{(1)}(y_s)^3\right] \\ &= \left[z_{xxx}^{(i)}(x_s)^3 + 3z_{xxy}^{(i)}(x_s)^2 y_s + 3z_{xyy}^{(i)}x_s(y_s)^2 + z_{yyy}^{(i)}(y_s)^3\right]. \end{aligned} \tag{18}$$

Letting s=0, we have from eq. (9) that

$$\begin{aligned} \dot{\kappa}_n^{(1)}\big|_\beta &= z_{xxx}^{(1)}\cos^3\beta + 3z_{xxy}^{(1)}\cos^2\beta\sin\beta \\ &\quad + 3z_{xyy}^{(1)}\cos\beta\sin^2\beta + z_{yyy}^{(1)}\sin^3\beta\big|_{x=0,y=0} \\ &= \dot{\kappa}_n^{(i)}\big|_\beta \\ &= z_{xxx}^{(i)}\cos^3\beta + 3z_{xxy}^{(i)}\cos^2\beta\sin\beta \\ &\quad + 3z_{xyy}^{(i)}\cos\beta\sin^2\beta + z_{yyy}^{(i)}\sin^3\beta\big|_{x=0,y=0}. \end{aligned} \tag{19}$$

Considering eqs. (14) and (19), we get the following proposition.

Proposition 2. Given a pair of line contact surfaces, at any point on the contact line a pair of normal sections can be determined according to the tangent direction of the contact line. The two normal sections have the same normal curvature and normal curvature derivative (with respect to the arc length) at that point.

2.4 Properties of a pair of second-order line contact surfaces

If the cutter envelope surface and design surface have the second order contact at any point on the CC path $\boldsymbol{r}^{(1)}(s)=\boldsymbol{r}^{(2)}(s)$, then we have

$$\begin{cases} \dfrac{z_{xx}^{(1)}(s)}{\sqrt{1+(z_x^{(1)})^2+(z_y^{(1)})^2}} = \dfrac{z_{xx}^{(2)}(s)}{\sqrt{1+(z_x^{(2)})^2+(z_y^{(2)})^2}}, \\ \dfrac{z_{xy}^{(1)}(s)}{\sqrt{1+(z_x^{(1)})^2+(z_y^{(1)})^2}} = \dfrac{z_{xy}^{(2)}}{\sqrt{1+(z_x^{(2)})^2+(z_y^{(2)})^2}}, \\ \dfrac{z_{yy}^{(1)}(s)}{\sqrt{1+(z_x^{(1)})^2+(z_y^{(1)})^2}} = \dfrac{z_{yy}^{(2)}}{\sqrt{1+(z_x^{(2)})^2+(z_y^{(2)})^2}}. \end{cases} \tag{20}$$

According to eqs. (12) and (20), we have

$$\begin{cases} z_{xx}^{(1)}(s) = z_{xx}^{(2)}(s), \\ z_{xy}^{(1)}(s) = z_{xy}^{(2)}(s), \\ z_{yy}^{(1)}(s) = z_{yy}^{(2)}(s). \end{cases} \tag{21}$$

Taking the derivatives of both sides of eq. (21) with respect to arc length s, we obtain

$$\begin{cases} z_{xxx}^{(1)}x_s + z_{xxy}^{(1)}y_s = z_{xxx}^{(2)}x_s + z_{xxy}^{(2)}y_s, \\ z_{xyx}^{(1)}x_s + z_{xyy}^{(1)}y_s = z_{xyx}^{(2)}x_s + z_{xyy}^{(2)}y_s, \\ z_{yyx}^{(1)}x_s + z_{yyy}^{(1)}y_s = z_{yyx}^{(2)}x_s + z_{yyy}^{(2)}y_s. \end{cases} \tag{22}$$

Letting s=0, we get

$$\begin{cases} z_{xxx}^{(1)}\cos\beta + z_{xxy}^{(1)}\sin\beta\big|_{x=0,y=0} = z_{xxx}^{(2)}\cos\beta + z_{xxy}^{(2)}\sin\beta\big|_{x=0,y=0}, \\ z_{xyx}^{(1)}\cos\beta + z_{xyy}^{(1)}\sin\beta\big|_{x=0,y=0} = z_{xyx}^{(2)}\cos\beta + z_{xyy}^{(2)}\sin\beta\big|_{x=0,y=0}, \\ z_{yyx}^{(1)}\cos\beta + z_{yyy}^{(1)}\sin\beta\big|_{x=0,y=0} = z_{yyx}^{(2)}\cos\beta + z_{yyy}^{(2)}\sin\beta\big|_{x=0,y=0}. \end{cases} \tag{23}$$

3 Local reconstruction of the cutter envelope surface

3.1 Second-order reconstruction

As shown in Figure 3, the cutter envelope surface contacts with the design surface along the CC path. From eq. (16), we have

$$\begin{cases} z_{xx}^{(1)}\cos\alpha + z_{xy}^{(1)}\sin\alpha\big|_{x=0,y=0} = z_{xx}^{(2)}\cos\alpha + z_{xy}^{(2)}\sin\alpha\big|_{x=0,y=0}, \\ z_{yx}^{(1)}\cos\alpha + z_{yy}^{(1)}\sin\alpha\big|_{x-0,y=0} = z_{yx}^{(2)}\cos\alpha + z_{yy}^{(2)}\sin\alpha\big|_{x-0,y=0}, \end{cases} \tag{24}$$

where α is the angle between the tangent of the CC path at $\boldsymbol{r}_0$ and the x-axis of the local frame. As shown in Figure 4, the cutter envelope surface and the cutter surface at the current location are tangent along the characteristic curve. From Proposition 2 and eq. (14), we have

$$\kappa_n^{(0)}\big|_\beta = z_{xx}^{(1)}\cos^2\beta + 2z_{xy}^{(1)}\cos\beta\sin\beta + z_{yy}^{(1)}\sin^2\beta\big|_{x=0,y=0}, \tag{25}$$

where β denotes the angle between the tangent of the characteristic curve at $\boldsymbol{r}_0$ and the x-axis of the local frame. Combining eqs. (24) and (25), we obtain

$$\begin{bmatrix} \cos\alpha & \sin\alpha & 0 \\ 0 & \cos\alpha & \sin\alpha \\ \cos^2\beta & 2\cos\beta\sin\beta & \sin^2\beta \end{bmatrix}\begin{bmatrix} z_{xx}^{(1)} \\ z_{xy}^{(1)} \\ z_{yy}^{(1)} \end{bmatrix} = \begin{bmatrix} z_{xx}^{(2)}\cos\alpha + z_{xy}^{(2)}\sin\alpha \\ z_{yx}^{(2)}\cos\alpha + z_{yy}^{(2)}\sin\alpha \\ \kappa_n^{(0)}\big|_\beta \end{bmatrix}. \tag{26}$$

The tangent direction of the CC path is also referred to as the cutting direction. If it is along the x-axis, i.e. $\alpha = 0$, eq. (26) becomes

$$\begin{bmatrix} 1 & 0 & 0 \\ 0 & 1 & 0 \\ \cos^2\beta & 2\cos\beta\sin\beta & \sin^2\beta \end{bmatrix}\begin{bmatrix} z_{xx}^{(1)} \\ z_{xy}^{(1)} \\ z_{yy}^{(1)} \end{bmatrix} = \begin{bmatrix} z_{xx}^{(2)} \\ z_{xy}^{(2)} \\ \kappa_n^{(0)}\big|_\beta \end{bmatrix}. \tag{27}$$

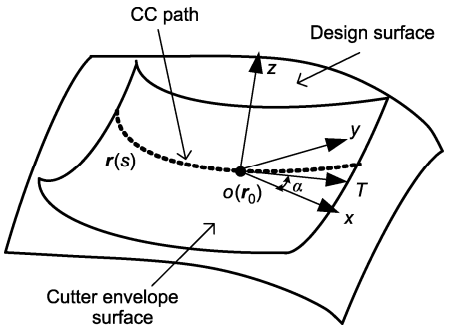

Figure 3 Line contact between the cutter envelope surface and design surface (along the CC path).

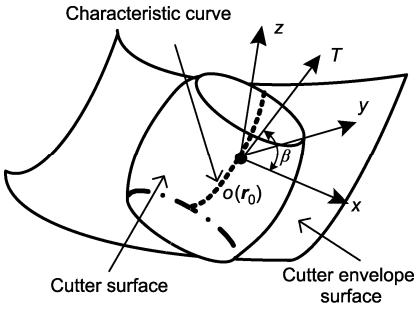

Figure 4 Line contact between the cutter envelope surface and cutter surface (along the characteristic curve).

Solving eq. (27) and considering eq. (14), we get

$$\begin{cases} z_{xx}^{(1)} - z_{xx}^{(2)} = 0, \\ z_{xy}^{(1)} - z_{xy}^{(2)} = 0, \\ z_{yy}^{(1)} - z_{yy}^{(2)} = (\kappa_n^{(0)} - \kappa_n^{(2)})\big|_\beta / \sin^2\beta. \end{cases} \tag{28}$$

Then, it follows from eq. (8) that

$$(\kappa_n^{(1)} - \kappa_n^{(2)})\big|_\gamma = \frac{(\kappa_n^{(0)} - \kappa_n^{(2)})\big|_\beta \sin^2\gamma}{\sin^2\beta}, \tag{29}$$

where γ denotes the angle between a specified surface tangent at point $\boldsymbol{r}_0$ and the x-axis of the local frame, which is along the cutting direction. In differential geometry, the quantity $\kappa_n^{(1)} - \kappa_n^{(2)}$ is termed the relative normal curvature. Eq. (29) suggests the following proposition.

Proposition 3. The relative normal curvature between the cutter envelope surface and design surface at the CC point has the maximum value along the tangent direction perpendicular to the cutting direction. The cutter envelope surface and design surfaces have a second-order contact at the CC point if and only if they have the same normal curvature along the tangent direction of the characteristic curve of the cutter envelope surface.

3.2 Third-order reconstruction

If the cutter envelope surface and design surface have the second order contact at any point on the CC path, from eq. (23) we have

$$\begin{cases} (z_{xxx}^{(1)} - z_{xxx}^{(2)})\cos\alpha + (z_{xxy}^{(1)} - z_{xxy}^{(2)})\sin\alpha\big|_{x=0,y=0} = 0, \\ (z_{xyx}^{(1)} - z_{xyx}^{(2)})\cos\alpha + (z_{xyy}^{(1)} - z_{xyy}^{(2)})\sin\alpha\big|_{x=0,y=0} = 0, \\ (z_{yyx}^{(1)} - z_{yyx}^{(2)})\cos\alpha + (z_{yyy}^{(1)} - z_{yyy}^{(2)})\sin\alpha\big|_{x=0,y=0} = 0. \end{cases} \tag{30}$$

Following Proposition 2 and eq. (19), we have

$$\dot{\kappa}_n^{(0)}\big|_\beta = z_{xxx}^{(1)}\cos^3\beta + 3z_{xxy}^{(1)}\cos^2\beta\sin\beta + 3z_{xyy}^{(1)}\cos\beta\sin^2\beta + z_{yyy}^{(1)}\sin^3\beta\big|_{x=0,y=0}. \tag{31}$$

Combining eqs. (30) and (31), we obtain

$$\begin{bmatrix} \cos\alpha & \sin\alpha & 0 & 0 \\ 0 & \cos\alpha & \sin\alpha & 0 \\ 0 & 0 & \cos\alpha & \sin\alpha \\ \cos^3\beta & 3\cos^2\beta\sin\beta & 3\cos\beta\sin^2\beta & \sin^3\beta \end{bmatrix} \begin{bmatrix} z_{xxx}^{(1)} \\ z_{xxy}^{(1)} \\ z_{xyy}^{(1)} \\ z_{yyy}^{(1)} \end{bmatrix}$$

$$= \begin{bmatrix} z_{xxx}^{(2)}\cos\alpha + z_{xxy}^{(2)}\sin\alpha \\ z_{xxy}^{(2)}\cos\alpha + z_{xyy}^{(2)}\sin\alpha \\ z_{yyx}^{(2)}\cos\alpha + z_{yyyy}^{(2)}\sin\alpha \\ \dot{\kappa}_n^{(0)}\big|_\beta \end{bmatrix}. \tag{32}$$

Again, if the x-axis of the local frame is along the cutting direction, eq. (32) becomes

$$\begin{bmatrix} 1 & 0 & 0 & 0 \\ 0 & 1 & 0 & 0 \\ 0 & 0 & 1 & 0 \\ \cos^3\beta & 3\cos^2\beta\sin\beta & 3\cos\beta\sin^2\beta & \sin^3\beta \end{bmatrix} \begin{bmatrix} z_{xxx}^{(1)} \\ z_{xxy}^{(1)} \\ z_{xyy}^{(1)} \\ z_{yyy}^{(1)} \end{bmatrix}$$

$$= \begin{bmatrix} z_{xxx}^{(2)} \\ z_{xxy}^{(2)} \\ z_{yyx}^{(2)} \\ \dot{\kappa}_n^{(0)}\big|_\beta \end{bmatrix}. \tag{33}$$

Solving eq. (33) and considering eq. (19), we get

$$\begin{cases} z_{xxx}^{(1)} - z_{xxx}^{(2)} = 0, \\ z_{xxy}^{(1)} - z_{xxy}^{(2)} = 0, \\ z_{yyx}^{(1)} - z_{yyx}^{(2)} = 0, \\ z_{yyy}^{(1)} - z_{yyy}^{(2)} = \dfrac{(\dot{\kappa}_n^{(0)} - \dot{\kappa}_n^{(2)})\big|_\beta}{\sin^3\beta}. \end{cases} \tag{34}$$

Then, it follows from eq. (8) that

$$(\dot{\kappa}_n^{(1)} - \dot{\kappa}_n^{(2)})\big|_\gamma = \frac{(\dot{\kappa}_n^{(0)} - \dot{\kappa}_n^{(2)})\big|_\beta \sin^3\gamma}{\sin^3\beta}. \tag{35}$$

It suggests the following proposition.

Proposition 4. The derivative of the relative normal curvature between the cutter envelope surface and design surface at the CC point has the maximum value along the tangent direction perpendicular to the cutting direction. The cutter envelope surface and design surfaces have a third-order contact at the CC point if and only if they have the same normal curvature and normal curvature derivative along the tangent direction of the characteristic curve of the cutter envelope surface.

Eqs. (29) and (35) characterize the relationship among the cutter surface, cutter envelope surface and design surface in the neighborhood of the CC point. Although the cutter envelope surface can not be completely constructed given only one CL, its third-order approximation can be obtained. It is shown that at the CC point both the normal curvature of the normal section of the cutter envelope surface and its derivative with respect to the arc length of the normal section can be determined by those of the cutter surface and design surface. NC machining is a process that subtracts the swept volume generated by the cutter moving along the programmed tool paths from the current raw stock. Since the swept volume is enclosed by the swept envelope, which represents the set of points on the moving cutter that also lie on the machined surface, from the viewpoint of geometric simulation, the envelope surface of the cutter can be treated as the machined surface. Obviously, the machined surface is required to approximate to the design surface as much as possible. So, in cutter position optimization, it is desired to adjust the cutter location to minimize the objective function $|(\dot{\kappa}_n^{(0)} - \dot{\kappa}_n^{(2)})|_\beta / \sin^3\beta|$ under the constraint $\kappa_n^{(0)}|_\beta = \kappa_n^{(2)}|_\beta$ that guarantees the second-order point contact between the cutter envelope surface and design surface. The detailed model and algorithm will be addressed in part II of the paper. In ref. [15], a series of formulas were given to analytically calculate $\dot{\kappa}^{(i)}|_\theta$. Therefore, $\dot{\kappa}^{(i)}|_\theta$ can be easily obtained according to the direction of the surface normal at the CC point. Now the remaining question is how to determine the tangent direction of the characteristic curve of the cutter envelope surface, which is required by eqs. (29) and (35).

3.3 Tangent direction of the characteristic curve

Denote by $\kappa_{nx}^{(i)}$ and $\tau_{gx}^{(i)}$ the normal curvature and geodesic torsion of surface $\boldsymbol{r}^{(i)}$ at point $\boldsymbol{r}_0$ along the x-axis, and $\kappa_{ny}^{(i)}$ the normal curvature along the y-axis. Following Euler's and Bertrand's formulas, we have

$$\begin{cases} \kappa_n^{(i)} = \kappa_{nx}^{(i)}\cos^2\gamma + \kappa_{ny}^{(i)}\sin^2\gamma + \tau_{gx}^{(i)}\sin 2\gamma, \\ \tau_g^{(i)} = \dfrac{\kappa_{ny}^{(i)} - \kappa_{nx}^{(i)}}{2}\sin 2\gamma + \tau_{gx}^{(i)}\cos 2\gamma, \end{cases} \tag{36}$$

where γ is the angle between a specified surface tangent and the x-axis, and $\kappa_n^{(i)}$ and $\tau_g^{(i)}$ are the normal curvature and geodesic torsion along that tangent direction, respectively. Denote by α the angle between the tangent of the CC path and the x-axis, and β the angle between the tangent of the characteristic curve and the x-axis. The cutter envelope surface contacts with the design surface and cutter surface along the CC path and characteristic curve, respectively. Hence, the cutter envelope surface and the design or cutter surface have the same normal curvature and geodesic torsion at the CC point along the tangent direction of the CC

path or characteristic curve. Thus, we have

$$\begin{cases} \kappa_{nx}^{(1)}\cos^2\alpha+\kappa_{ny}^{(1)}\sin^2\alpha+\tau_{gx}^{(1)}\sin 2\alpha \\ \quad=\kappa_{nx}^{(2)}\cos^2\alpha+\kappa_{ny}^{(2)}\sin^2\alpha+\tau_{gx}^{(2)}\sin 2\alpha, \\ \dfrac{\kappa_{ny}^{(1)}-\kappa_{nx}^{(1)}}{2}\sin 2\alpha+\tau_{gx}^{(1)}\cos 2\alpha \\ \quad=\dfrac{\kappa_{ny}^{(2)}-\kappa_{nx}^{(2)}}{2}\sin 2\alpha+\tau_{gx}^{(2)}\cos 2\alpha, \end{cases} \tag{37}$$

$$\begin{cases} \kappa_{nx}^{(1)}\cos^2\beta+\kappa_{ny}^{(1)}\sin^2\beta+\tau_{gx}^{(1)}\sin 2\beta \\ \quad=\kappa_{nx}^{(0)}\cos^2\beta+\kappa_{ny}^{(0)}\sin^2\beta+\tau_{gx}^{(0)}\sin 2\beta, \\ \dfrac{\kappa_{ny}^{(1)}-\kappa_{nx}^{(1)}}{2}\sin 2\beta+\tau_{gx}^{(1)}\cos 2\beta \\ \quad=\dfrac{\kappa_{ny}^{(0)}-\kappa_{nx}^{(0)}}{2}\sin 2\beta+\tau_{gx}^{(0)}\cos 2\beta. \end{cases} \tag{38}$$

If the tangent direction of the CC path, or the cutting direction, is along the x-axis, i.e. α=0, eq. (37) becomes

$$\begin{cases} \kappa_{nx}^{(1)}=\kappa_{nx}^{(2)}, \\ \tau_{gx}^{(1)}=\tau_{gx}^{(2)}. \end{cases} \tag{39}$$

Substituting eq. (39) into eq. (38) results in

$$\begin{cases} \kappa_{nx}^{(2)}\cos^2\beta+\kappa_{ny}^{(1)}\sin^2\beta+\tau_{gx}^{(2)}\sin 2\beta \\ \quad=\kappa_{nx}^{(0)}\cos^2\beta+\kappa_{ny}^{(0)}\sin^2\beta+\tau_{gx}^{(0)}\sin 2\beta, \\ \dfrac{\kappa_{ny}^{(1)}-\kappa_{nx}^{(2)}}{2}\sin 2\beta+\tau_{gx}^{(2)}\cos 2\beta \\ \quad=\dfrac{\kappa_{ny}^{(0)}-\kappa_{nx}^{(0)}}{2}\sin 2\beta+\tau_{gx}^{(0)}\cos 2\beta. \end{cases} \tag{40}$$

Let $\kappa_{nx}^{(20)}=\kappa_{nx}^{(2)}-\kappa_{nx}^{(0)}$, $\kappa_{ny}^{(10)}=\kappa_{ny}^{(1)}-\kappa_{ny}^{(0)}$ and $\tau_{gx}^{(20)}=\tau_{gx}^{(2)}-\tau_{gx}^{(0)}$, which are referred to as the relative normal curvatures along the x- and y-axes and the relative geodesic torsion along the x-axis. Then, eq. (40) becomes

$$\begin{cases} \kappa_{nx}^{(20)}\cos^2\beta+\kappa_{ny}^{(10)}\sin^2\beta+\tau_{gx}^{(20)}\sin 2\beta=0, \\ \dfrac{\kappa_{ny}^{(10)}-\kappa_{nx}^{(20)}}{2}\sin 2\beta+\tau_{gx}^{(20)}\cos 2\beta=0. \end{cases} \tag{41}$$

Solving eq. (41), we get

$$\begin{cases} \tan\beta=-\dfrac{\kappa_{nx}^{(20)}}{\tau_{gx}^{(20)}}, \\ \kappa_{ny}^{(10)}=\dfrac{(\tau_{gx}^{(20)})^2}{\kappa_{nx}^{(20)}}. \end{cases} \tag{42}$$

It follows from eqs. (36) and (39) that

$$(\kappa_n^{(1)}-\kappa_n^{(2)})\Big|_\gamma=(\kappa_{ny}^{(1)}-\kappa_{ny}^{(2)})\sin^2\gamma. \tag{43}$$

Substituting the expression of $\kappa_{ny}^{(10)}$ in eq. (42) into eq. (43) leads to

$$(\kappa_n^{(1)}-\kappa_n^{(2)})\Big|_\gamma=\frac{\kappa_{nx}^{(02)}\kappa_{ny}^{(02)}-(\tau_{gx}^{(20)})^2}{\kappa_{nx}^{(02)}}\sin^2\gamma=\frac{K^{(02)}}{\kappa_{nx}^{(02)}}\sin^2\gamma, \tag{44}$$

where $K^{(02)}=\kappa_{nx}^{(02)}\kappa_{ny}^{(02)}-(\tau_{gx}^{(20)})^2$ is termed the relative Gauss curvature between two point contact surfaces [16]. According to the classification of the surface contact types [16], if $K^{(02)}=0$, at least one of the relative Gauss principal curvatures is zero. The two surfaces have a second-order contact if both of the relative Gauss principal curvatures are zero, and they are a pair of linear contact surfaces if only one of the relative Gauss principal curvatures is zero. Therefore, Proposition 3 can be equivalently expressed as follows.

Proposition 5. The cutter envelope surface and design surface have the second-order contact at the CC point if and only if the cutter surface and design surface are a pair of linear contact surfaces there.

It is seen that the condition that the cutter envelope surface has a second-order contact with the design surface is much weaker than the condition that the cutter surface has a second-order contact with the design surface. Although most of the results presented above have been reported in ref. [14], our derivations and descriptions are much simpler.

4 Cutter envelope surface reconstruction for flat-ended or disc cutter

When machining with flat-ended or disc cutters, the cutter surface degenerates into a circle, which is termed the cutting circle. The cutter envelope surface then degenerates into a pipe surface generated by the cutting circle undergoing a spatial motion. In this situation, eqs. (29) and (35) are invalid. New formulas need to be developed. In what follows, for simplification of the derivation it is assumed that the tangent direction of the CC path at the designated CC point is along the x-axis of the local frame.

4.1 Second-order reconstruction

According to eq. (16), we have

$$\begin{cases} z_{xx}^{(1)}=z_{xx}^{(2)}, \\ z_{xy}^{(1)}=z_{xy}^{(2)}. \end{cases} \tag{45}$$

It follows from eq. (8) that

$$(\kappa_n^{(1)}-\kappa_n^{(2)})\Big|_\gamma=(z_{yy}^{(1)}-z_{yy}^{(2)})\sin^2\gamma=\frac{(\kappa_n^{(1)}-\kappa_n^{(2)})\Big|_\beta\sin^2\gamma}{\sin^2\beta}, \tag{46}$$

where β is the angle between the tangent of the cutting cir-

cle at the CC point and the *x*-axis of the local frame, as illustrated in Figure 5. Denote by η the angle between the plane that the cutting circle lies on and the *x*-*y* plane. According to Meusnier theorem, we have

$$\kappa_n^{(1)}\Big|_\beta = \frac{\sin\eta}{R}, \tag{47}$$

where *R* stands for the radius of the cutting circle. Since $\kappa_n^{(2)}\Big|_\beta$ can be accurately calculated, the relative normal curvature between the cutter envelope surface and design surface at the CC point along any tangent direction can be determined according to eq. (46).

4.2 Third-order reconstruction

According to eq. (23), we have

$$\begin{cases} z_{xxx}^{(1)} = z_{xxx}^{(2)}, \\ z_{xyx}^{(1)} = z_{xyx}^{(2)}, \\ z_{yyx}^{(1)} = z_{yyx}^{(2)}. \end{cases} \tag{48}$$

It follows from eq. (9) that

$$(\dot\kappa_n^{(1)} - \dot\kappa_n^{(2)})\Big|_\gamma = (z_{yyy}^{(1)} - z_{yyy}^{(2)})\sin^3\gamma = \frac{(\dot\kappa_n^{(1)} - \dot\kappa_n^{(2)})\Big|_\beta \sin^3\gamma}{\sin^3\beta}. \tag{49}$$

Since $\dot\kappa_n^{(2)}\Big|_\beta$ can be accurately calculated, the remaining problem is to solve for $\dot\kappa_n^{(1)}\Big|_\beta$. The plane that the cutting circle lies on can be implicitly expressed as $z = \tan\eta(y\cos\beta - x\sin\beta)$. A section curve is obtained by intersecting this plane with the cutter envelope surface. The derivative of the curvature of this planar curve with respect to its arc length at the CC point has the expression

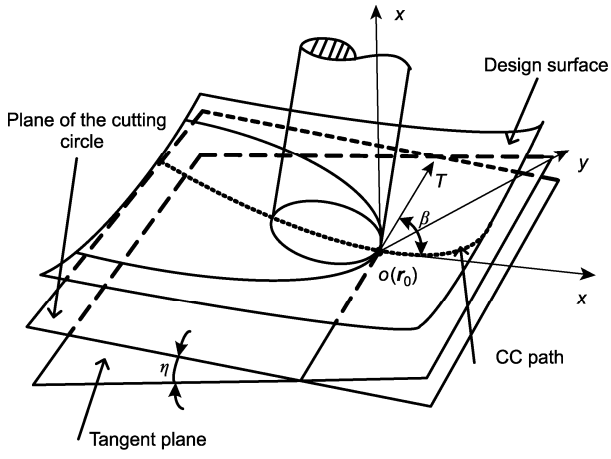

Figure 5 Point contact between the base circle and design surface.

$$\kappa_s = \frac{z_{xxx}^{(1)}\cos^3\beta + 3z_{xxy}^{(1)}\cos^2\beta\sin\beta + 3z_{xyy}^{(1)}\cos\beta\sin^2\beta + z_{yyy}^{(1)}\sin^3\beta}{\sin\eta} + \frac{3(z_{xx}^{(1)}\cos^2\beta + 2z_{xy}^{(1)}\cos\beta\sin\beta + z_{yy}^{(1)}\sin^2\beta)\tau_{g\beta}^{(1)}\cos\eta}{\sin^2\eta}, \tag{50}$$

where $\tau_{g\beta}^{(1)}$ denotes the geodesic torsion of the cutter envelope surface along the tangent direction of the cutting circle at the CC point. It was proved in ref. [16] that the pair of second order line contact surfaces had the same principal directions and principal curvatures at any point on the contact line. Therefore, we have $\tau_{g\beta}^{(1)} = \tau_{g\beta}^{(2)}$. Then, according to eqs. (8) and (9), eq. (50) can be re-formulated as

$$\kappa_s = \frac{\dot\kappa_n^{(1)}\Big|_\beta}{\sin\eta} + \frac{3\kappa_n^{(1)}\Big|_\beta \tau_{g\beta}^{(2)}\cos\eta}{\sin^2\eta} = \frac{\dot\kappa_n^{(1)}\Big|_\beta}{\sin\eta} + \frac{3\tau_{g\beta}^{(2)}\cos\eta}{R\sin\eta}. \tag{51}$$

The intersection of the plane that the cutting circle lies on with the cutter envelope surface yields the cutting circle itself, which means that κ_s=0. Therefore, we have

$$\dot\kappa_n^{(1)}\Big|_\beta = -\frac{3\tau_{g\beta}^{(2)}\cos\eta}{R}. \tag{52}$$

Now, the derivative of the relative normal curvature between the cutter envelope surface and design surface at the CC point along any tangent direction can be determined according to eq. (49).

5 Conclusions

The geometric properties of a pair of line contact surfaces are investigated. Based on the observation that the cutter envelope surface contacts with the cutter surface and design surface along the characteristic curve and CC path, respectively, a mathematical model describing the third-order approximation of the cutter envelope surface according to just one given CL is developed. It is shown that the cutter envelope surface has a third-order contact with the design surface at the CC point if and only if they have the same normal curvature and normal curvature derivative along the tangent direction of the characteristic curve of the cutter envelope surface. The model characterizes the intrinsic relationship among the cutter surface, cutter envelope surface and design surface in the neighborhood of the CC point, and yields the mathematical foundation for optimally approximating the cutter envelope surface to the design surface by adjusting the cutter location. It applies to general rotary cutters and complex surfaces.

This work was supported by the National Natural Science Foundation of China (Grant Nos. 50835004, 50775147), the National Basic Research Program of China ("973" Program) (Grant No. 2005CB724103) and the Science & Technology Commission of Shanghai Municipality (Grant No. 07JC14028). The authors would like to thank Dr. Hu Gong for the valuable discussions with him.

1 Zhu L M, Zheng G, Ding H. Formulating the swept envelope of rotary cutter undergoing general spatial motion for multi-axis NC machining. Int J Mach Tool Manu, 2009, 49(2): 199–202
2 Zhu L M, Zhang X M, Zheng G, et al. Analytical expression of the swept surface of a rotary cutter using the envelope theory of sphere congruence. J Manuf Sci E-T ASME, 2009, 131(4): 041017-1–041017-7
3 Deng Z, Leu M C, Wang L, et al. Determination of flat-end cutter orientation in 5-axis machining. ASME Med, 1996, 4: 73–80
4 Kruth J P, Klewais P. Optimization and dynamic adaptation of the cutter inclination during five-axis milling of sculptured surfaces. CIRP Ann-Manuf Tech, 1994, 43(1): 443–448
5 Rao N, Bedi S, Buchal R. Implementation of the principal-axis method for machining of complex surfaces. Int J Adv Manuf Tech, 1996, 11(4): 249–257
6 Bedi S, Gravelle S, Chen Y H. Principal curvature alignment technique for machining complex surface. J Manuf Sci E-T ASME, 1997, 119(4B): 756–765
7 Warkentin A, Ismail F, Bedi S. Multi-point tool positioning strategy for 5-axis machining of sculptured surfaces. Comput Aided Geom D, 2000, 17(1): 83–100
8 Chiou C J, Lee Y S. A machining potential field approach to tool path generation for multi-axis sculptured surface machining. Comput Aided Design, 2002, 34(5): 357–371
9 Ni Y R, Ma D Z, Zhang H, et al. Optimal orientation control for torus tool 5-axis sculptured surface NC machining (in Chinese). Chinese J Mech Eng, 2001, 37(2): 87–90
10 Cao L X, Wu H J, Liu J. Geometrical theory of machining free form surface by cylindrical cutter in 5-axis NC machine tools (in Chinese). Chinese J Mech Eng, 2003, 39(7): 134–137
11 Wang X C, Wu X T, Li Y B. Curvature catering—A new concept for machining sculptured surfaces (in Chinese). J Xi'an Jiaotong Univ, 1992, 26(5): 51–58
12 Rao A, Sarma R. On local gouging in five-axis sculptured surface machining using flat-end tools. Comput Aided Design, 2000, 32(7): 409–420
13 Yoon J H, Pottmann H, Lee Y S. Locally optimal cutting positions for 5-axis sculptured surface machining. Comput Aided Design, 2003, 35(1): 69–81
14 Gong H, Cao L X, Liu J. Second order approximation of tool envelope surface for 5-axis machining with single point contact. Comput Aided Design, 2008, 40(5): 604–615
15 He N X, Li S D. Curvature tensor and curvature derivative tensor of conjugate surfaces (in Chinese). Chinese J Mech Eng, 1979, 15(3-4): 93–108
16 Cao L X, Gong H, Liu J. Research on contact problem of surfaces and contact characteristics of offset surfaces (in Chinese). J Dalian Univ Technol, 2007, 47(1): 39–44